CLAY SETTLING IN FRESH AND SALT WATER

BRUCE R. SUTHERLAND[1,2], KAI J. BARRETT[1] and MURRAY K. GINGRAS[2]

[1]Department of Physics, University of Alberta, Edmonton, Alberta T6G 2E1, Canada

[2]Department of Earth and Atmospheric Sciences, University of Alberta, Edmonton, Alberta T6G 2E3, Canada

ABSTRACT: To gain insight into the process of sedimentation occurring when clay-laden estuaries and deltas enter marine water, we perform laboratory experiments to measure the settling rate of Kaolin clay in fresh and salt water. In fresh water, sedimentation is a slow process with the clay particle concentration gradually decreasing nearly uniformly within the 10 cm deep tank over hours. The dynamics are dramatically different for clay setting in salt water with salinities between 20 psu and 70 psu. Within minutes the clay particles flocculate and a sharp front between clay-laden and clear water forms near the surface. After formation the front descends at near constant rate such that the 10 cm deep tank is cleared of particles in minutes instead of hours. We measure the initial speed of descent of the front as it depends upon salinity and clay concentration. The descent rate is found to be independent of salinity provided it exceeds 20 psu. However, the descent velocity, v, decreases with increasing concentration, C, according to a power law: v propto C^(-1.7). The consequences for understanding sedimentation from river plumes are discussed.

INTRODUCTION

In natural settings, flocculation of clay minerals occurs dominantly in estuaries and deltas where fluvial (i.e. approximately 0 psu) waters are mixed with marine waters (approximately 30 psu). This process of sedimentation is of interest as it strongly

influences the distribution of fine-grained sediment in these marginal-marine locales. Importantly, parameterizing mud-bed sedimentation can help to interpret mud-rock distribution in the stratigraphic record. For example, within estuaries the inner half is more prone to hosting clay-dominated strata. In contrast, deltas export mud to the delta front and prodelta.

Herein we present the results of simple experiments that provide insight into the influence of salinity upon flocculation and settling of clay particles. The experiments provide repeatable observations, are inexpensive and the experimental apparatus is easily constructed. The experimental results allow us to develop an empirical model characterizing the influence salinity has on the settling of inorganic particles as a result of enhancing the flocculation and sedimentation of clay, a process that contributes to the deposition of mud beds where rivers first interact with sea water in estuaries and deltas. We also show that increasing the salinity beyond a nominal value does not change the settling rate whereas this rate is retarded as particle concentrations become large as in the benthic layer and at delta fronts.

Through a mix of laboratory experiments and observations, several models have been proposed for the deposition (as well as erosion) rate of fines in turbulent shear flow. Generally these assume the deposition rate is proportional to concentration, C, of particles and the settling velocity, w_s (Krone 1962; Parchure and Mehta 1985; Lau and Krishnappan 1994; Krone 1993; Sanford and Halka 1993; Winterwerp 2006). Specifically, in the study of Winterwerp (2006), the deposition rate was shown to be

given simply by their product: $D=w_s C_b$ in which w_s depends upon time but not depth and C_b is the near-bottom concentration. The laboratory experiments, designed to study the simultaneous processes of deposition and erosion, were performed in flume tanks with particles premixed with saline water. As such they did not focus specifically upon deposition as it depends upon salinity and concentration in the absence of turbulent stresses.

Oligohaline (0.5-5 psu) and mesohaline salinities (5-18 psu) are broadly accepted to induce flocculation and clay settling (e.g. Eisma and Cadee 1991; Ani et al 1991; Uncles et al 2006). This corresponds well to studies in modern estuaries, where the turbidity maximum zone is normally positioned within the inner estuary, and where salinities are characteristically below 10 psu (e.g. Gingras et al 1999; Uncles et al 2006). For example, in the study of Chesapeake Bay by Cercoa et al (2013), the summertime turbidity maxima for the northern and northeastern estuary reaches occur approximately in the range 7.5 to 12.5 psu (in the winter salinity is approximately 5 psu lower in those areas). This is likely a result of enhanced flocculation and tidal resuspension in the area of pronounced flocculation. Suspended sediment content decreases in the seaward direction, which is interpreted to be a result of clay sedimentation in the inner estuary and dilution from sea water. The overall distribution of fine sediment is more complicated, in that some tributaries to Chesapeake Bay (e.g. the Choptank and Nanticoke rivers) contribute little in the way of fine sediment, and thus display no pronounced turbidity maximum. In contrast, the James River is closer to the bay mouth and its associated sediments are seaward of the other rivers.

A qualitative link between salinity and suspended inorganic sediment concentration is shown in Figure 1. The salinity (produced by the Chesapeake Bay Project) changes gradually from that of fresh water at the tips of the estuaries to values greater than 24 PSU, close to the values of salinity found in the open ocean. By contrast, the suspended sediment (computed by Cerco et al 2013) changes rapidly from concentrations greater than 25 ppt (parts per thousand by mass) to negligible concentrations within the main body of the estuary. Although the motion of tides and the seasonal changes in sediment discharge certainly affect the sediment concentration, these plots suggest a climatology in which sediments rapidly settle out of the fluid column when they become in contact with moderate salinity.

These trends in sediment distribution are not limited to Chesapeake Bay. They have been observed in the Gironde Estuary, France (Allen and Posamentier 1993), the Jiaojiang Estuary, China (Guan et al 2005, Fig. 5), and at Kouchibouguac Bay (Hauck et al 2009), to name a few.

Individual clay particles are plate-shaped with negative charges around their perimeter and positive charges in the center. This arrangement of charges is such that plates repel each other when dispersed in fresh water. However, if the water is saline, the sodium and chlorine ions act to neutralize the repulsive forces so that the plates may flocculate. Consequently, clay is expected to settle as flocs in salt water faster than as individual plates in fresh water. Indeed, clay settling in salt water qualitatively changes

the nature of the settling dynamics. When flocs form and settle, they sweep up smaller particles and flocs beneath them as they fall. Thus the incident flocs grow to larger size falling faster and more efficiently sweeping up smaller particles. This positive feedback leads to the formation of a descending front between near surface fresh water, which has been swept nearly clear of clay, and concentrated clay flocs (Couch and Hinch 1991).

These dynamics are demonstrated and settling rates quantified for the first time in the experiments reported upon here

SET-UP, ANALYSIS METHODS AND QUALITATIVE RESULTS

Experiments were performed in a rectangular tank with 0.5 cm thick acrylic side walls. The setup is sketched in Figure 2. The interior length and width of the tank was 20.0 cm and W=5.1 cm, respectively. The tank was 30 cm tall, but typically the depth of fluid in the tank was about H=10 cm. At the start of an experiment, the tank was filled to 10 cm with fresh water. A specified mass of salt (if any) was then mixed in and the resulting density measured to five-digit accuracy using an Anton Paar DMA 4500 density meter. Finally, a specified mass of dry kaolin clay was added to the salt water. The tank was stirred vigorously but briefly with a mixer until the mixture was uniform. The stirrer was extracted and this was taken to be the start time (t=0) of the experiment.

To visualize the evolution of the flow, a halogen light was placed well behind the tank and, to diffuse the lighting, a translucent white plastic sheet was placed against the back of the tank extending from the bottom to 10 cm height. Above this black construction paper was fastened between 10 cm and the top of the tank. Finally, a black cloth was draped over the setup between the camera lens and the tank. In this way, the only light that reached the camera passed through the mixture in the tank.

Experiments were recorded on a Sony Digital CCD camcorder. The shutter speed and iris were fixed so that the light intensity reaching the camera qualitatively measured the concentration of clay in the solution: low intensity indicated high light attenuation resulting from relatively high clay concentration; high intensity indicated relatively low clay concentration. The camera was placed 1.5 m from the front of the tank with its field of view spanning the height and most of the tank width.

Snapshots taken at three times from experiments with clay setting in fresh water and in salt water are shown in Figure 3. In experiments with moderate concentrations of salt and clay, we found that the clay descended over the water depth between 10 and 40 minutes. In solutions with salinities above 10psu, a front developed clearly delineating the separation between high and low clay concentration.

To track the front position in time, we sequentially examined frames from movies of the experiment. Each frame was imported into the image and data analysis software "MatLab" (www.mathworks.com) where the digitized intensities were represented by a

matrix. Averaging along each row produced a column of data representing the horizontally averaged intensity as a function of height. Concatenating this data determined at successive times, with a resolution of 1 second, we constructed vertical time series as shown, for example, in Figure 4.

The four vertical time series show the evolution of the system as the clay settles. We found there was a qualitative difference in behavior for clay setting in fresh and saline water. For clay in fresh water, the system remained well mixed while the overall concentration slowly decreased (e.g. see Fig. 4a). In most experiments, clay was still partially in suspension after being left overnight.

However, if the ambient was moderately saline, we observed the development of a front where the concentration of clay rapidly decreased with height. This front descended relatively rapidly so that most of the clay had fallen out of suspension within an hour. In cases with weak salinity, the front took some time to develop, but then descended rapidly (Fig. 4b). In experiments with greater salinity, the front formed relatively quickly and was relatively sharp, exhibiting a 50% intensity change from dark to light (from high to low clay concentration) over less than a centimeter height (Fig. 4c). The front was found to develop and descend most quickly if the clay concentrations were weak in sufficiently salty water. In such cases, however, the front was not so sharply defined (Fig. 4d).

To provide a quantitative measure of these observations, we characterized the formation time and descent of the front by superimposing contours of constant intensity on the vertical time series and determining the best-fit line over a fixed vertical range. The procedure is illustrated in Figure 5. This composite image shows the vertical time series of intensity as a gray scale except in the band between z=7 and 8 cm, which shows the intensity in false color.

Within the color band we find the minimum and maximum intensities, Imin and Imax, respectively. From these we compute the low, intermediate and high intensities given respectively by

$$I_L = 3/4\ I_{min} + 1/4\ I_{max},$$

$$I_0 = 1/2\ (I_{min} + I_{max}),$$

$$I_H = 1/4\ I_{min} + 3/4\ I_{max}.$$

The dashed white lines in Figure 5 show the contours of constant I_L, I_0 and I_H.

Within the range of the color band we find the best-fit line to each of the three contours. These are drawn in black on Figure 5 in the range 7<= z<= 8 cm. The magnitude of the average slopes of these three lines is used as a measure of the settling rate. The standard deviation of the three measurements gives an error estimate. In experiments with sharp fronts (as in Fig. 4c) we expect the error to be small because the three contours are closely packed together.

In Figure 5 the three best-fit lines are extrapolated to higher and lower depths as indicated by the long-dashed cyan lines. Where these lines intersect the surface at z=10 cm we have drawn circles. The average of the corresponding times where the circles are located denotes the virtual times at which the front would have begun to descend had it developed immediately and fallen at the measured settling rate. Again, the error determined from the three time measurements gives an indication of the spread of the front for 7<= z<= 8.

In our analysis, we found best-fit lines for z in the range between 7 and 8 cm in all but experiments with very weak salinity (S<=10 ppt). In these cases, a clearly defined front was not evident for long times and became manifest at lower depths. In these cases we applied the analysis procedure described above for 6<= z<= 7.

QUANTITATIVE RESULTS

We performed more than 50 experiments examining the settling of clay in fresh and salt water. In all experiments with fresh water, no front developed. Rather the concentration of clay gradually decreased in time while exhibiting little variation in the space. Even after more than 10 hours, a substantial concentration of clay particles remained in suspension.

In the analysis below, we focus on experiments examining clay settling in salt water. In such cases we can clearly identify a front between high and low-concentrations of clay

and we can record the formation time and descent rate of the front using analysis methods described in the previous section. By examining how the characteristics of the front change as the ambient salinity is reduced, we provide insight into the transition from fresh to saline dynamics.

Figure 6 shows the speed of descent of the front measured in experiments with different ambient salinities, S, measured in grams of salt per kilogram fresh water (i.e. parts-per-thousand (ppt) solute to solvent). Different symbols are plotted depending upon the concentration of clay, also measured in ppt (grams clay per kilogram fresh water).

The plot shows that at fixed clay concentration, the speed of descent of the front changes little with salinity provided S>10 ppt. The clay concentration is the most important factor in determining the front descent rate.

The vertical lines surrounding each point show the error in the speed measurement. These are large for experiments with weak concentrations of clay, but are negligible for C > 25 ppt. Thus, although the front descends quickly if C=14.7 ppt, it is more diffuse than the front in experiments with high clay concentrations. This is consistent with time series shown in Figure 4d.

From the intercepts of the best-fit lines with z=10 cm, we determine the average virtual start time for the front descent, as shown in Figure 7a. The same symbols are used as in Figure 6 to denote experiments with different clay concentrations. The plots shows

that, if the salinity is sufficiently large (S>10 ppt) and the concentration sufficiently high (C>25 ppt), the front forms almost immediately when the experiment begins. If the clay concentration is weaker, the front takes longer to develop and, as indicated by the extend of the error bars, it is more diffuse.

Significantly, if the salinity of the ambient is weak (S<10 ppt) the time for development of the front can take tens of minutes. The front itself is quite diffuse having errors in the virtual start time on the order of hundreds of seconds.

The implications for the descent rate and virtual start time measurements is succinctly represented in Figure 7b, in which an estimate of the settling time is given by computing the minimum settling time $T_0 + H/v$, in which T_0 is the virtual start time and H/v is the time for the front to descend over the depth H of the tank at speed v.

The fastest settling time (approximately 10 minutes) occurs for weak clay solutions (C<20 ppt) in moderately saline fluid (S>10 ppt). The settling time increases as the clay concentration increases because the front descent rate is smaller, even though the front takes less time to develop.

In weakly saline ambients, the settling time is very long because the front descends slowly and takes a long time to develop. In the limit of zero salinity, the front does not develop at all and setting is a long process.

In an attempt to synthesize these results together, Figure 8 plots the descent rate as a function of clay concentration. The descent rate is the average of the rates measured in experiments with fixed clay concentration and salinity ranging between 20 and 60 ppt.

The plot clearly shows the front speed decreasing as the concentration increases. When replotted on log-log axes (inset), we find the curve forms a straight line with slope -1.7. This gives an empirical measurement for the front descent rate of

$$v = v_0 \, (C/C_0)^{-1.7},$$

in which, somewhat arbitrarily, we have v_0=0.005 cm/s for C_0=40 ppt.

DISCUSSION AND CONCLUSIONS

The experimental results shed light on 3 aspects of mud sedimentation:

(1) they confirm and help parameterize the observation that clays readily flocculate at low salinities that are coincidental with salinity thresholds in estuaries;

(2) the data lead us to conclude that salinity increases above 10 psu do not increasingly promote sedimentation, suggesting that sediment-distribution patterns into higher salinity basins will be similar to those observed in estuaries;

(3) high sediment concentrations discourage flocculation and may offer another mechanism to consider when modeling offshore sediment transport in both hyperpycnal and hypopycnal plumes.

In general, our lab results are in accordance with studies of modern estuaries (Allen and Posamentier 1993; Guan et al 2005; Hauck et al 2009), which taken together suggest that most clay flocculation occurs at salinities near 10 psu.

The observation that settling rates are not noticeably increased in waters exceed 25 psu suggests that where sediment is delivered to marine basins, as in a delta, the resulting sediment plume, which is an important mechanism for delivering sediment to the shelf, can interact substantially with marine waters before flocculating. This may explain the longevity of large sediment plumes. The Amazon Shelf, for example, receives sediment at distances >1,400 km from the Amazon River Mouth (Gibbs 1977). Although a large volume of river discharge produces a salinity anomaly, tidal mixing influences the character of the basal salinity front resulting in a plume that is generally 5-10 m thick, with a salinity of 20-30 psu (Geyer et al 1996). Needless to say, if increasing salinities resulted in ever increasing flocculation rates, such delta plumes would be devoid of clay sediment.

The limited influence that increasing salinities have on flocculation rates is also a consideration where water enters hypersaline basins. In those situations clay should have similar distributions to that observed in brackish-water estuaries.

Also observed in the reported experiments is the tendency for settling rates to slow where the suspended-sediment load exceeds 10 g/L. In most estuary settings

suspended sediment ranges in the turbidity maximum fall well below this threshold. Many tributaries of Chesapeake Bay, as well as Willapa Bay, Tillamook Bay and Coos Bay (west coast USA), display approximately 1 g/L suspended sediment in the inner estuary (Uncles and Smith 2005). There are exceptions: the Amazon River estuary approaches 10 g/L (Geyer et al 1996); the Changjiang Estuary, in China ranges from 0.5 to 10 g/L (Shi and Kirby 2003); the Fly River delta in Papua New Guinea has a turbidity maximum of 10 g/L (Harris et al 2004); the Trent Estuary in the UK is approximately 12 g/l (Mitchell et al 2003); and the Gironde Estuary locally exceeds 12 g/l (Doxarana et al 2009). Notably in the examples cited above, all of the latter (i.e. high-suspended-sediment-load examples) export fine-sediment to the receiving oceanic basin, whereas the prior normally do not. This suggests that under conditions of high suspended-sediment loads, interference in the flocculation process is at least a factor in transporting clay to the ocean basin.

The impairment of flocculation due to high suspended-sediment concentration may also be a factor in delivering fluid muds to the shelf. Fluid mud deposits are increasingly identified in the rock record, and are broadly ascribed to delta-associated density currents comprising sediment-laden hyperpycnal flows derived from high-volume river discharge (see Bhattacharya and MacEachern (2009) for a complete treatment of the subject). The resulting density flow can travel long distances (Lamb and Mohrig 2009, and is thought to be an important process in transporting mud to the shelf. In all modern examples, the suspended sediment load exceeds 7 g /L (e.g. Waipaoa, NZ, 28 g/L Hicks et al 2004; the Fly River, PNG, 10 g/L, Harris et al 2004). Although speculative,

based on the data, it is reasonable to hypothesize that the coherence of fluid muds may be in part maintained by the diminished flocculation rate of clay in the marine basin.

REFERENCES

Allen, G. P. and Posamentier, H. W. 1993 Sequence stratigraphy and facies model of an incised valley fill; the Gironde Estuary, France: J. Sedimentary Petrology, v. 63 (3), p. 378-391.

Ani, S. A., Dyer, K. R. and Huntley, D. A. 1991 Measurement of the influence of salinity on floc density and strength:: Geo-Marine Letters, v. 11 (3-4), p. 154-158.

Cerco, C. F., Kim, S.-C. and Noel, M. R. 2013 Management modeling of suspended solids in the Chesapeake Bay, USA: Estuarine, Coastal and Shelf Science, v. 116, p. 87-98.

Couch, M. C. and Hinch, E. J. 1991 Sedimentation, Aggregation and compaction. In: Physics of Granular Media (ed. Bideau, D. and Dodds, J. A.), Nova Sciences Publishers, p. 299-321.

Doxarana, D., Froidefondb, J.-M., Castaingb, P. and Babina, M. 2009 Dynamics of the turbidity maximum zone in a macrotidal estuary (the Gironde, France): Observations from field and MODIS satellite data. : Estuarine, Coastal and Shelf Science, v. 81 (3), p. 321-332.

Eisma, D. and Cadee, G. C. 1991 Particulate matter processes in estuaries: SCOPE, v. 42, p. 283-296.

Geyer, W. R., Beardsley, R. C., Lentz, S. J., Candela, J., Limeburner, R., Johns, W. E. and Soares, I. D. 1996 Physical oceanography of the Amazon shelf: Continental Shelf Research, v. 16 (5-6), p. 575-616.

Gibbs, R. J. 1977 Clay mineral segregation in the marine environment: Journal of Sedimentary Petrology, v. 47 (1), p. 237-243.

Gingras, M. K., Pemberton, S. G., Saunders, T. and Clifton, H. E. 1999 The ichnology of modern and pleistocene brackish-water deposits at Willapa Bay, Washington; Variability in estuarine settings: Palaios, v. 14 (4), p. 352-374.

Guan, W. B., Kot, S. C. and Wolanski, E. 2005 3-D fluid-mud dynamics in the Jiaojiang Estuary, China: Estuarine, Coastal and Shelf Science, v. 65 (4), p. 747-762.

Harris, P. T., Hughes, M. G., Baker, E. K., Dalrymple, R. W. and Keene, J. B. 2004 Sediment transport in distributary channels and its export to pro-deltaic environment in a tidally dominated delta: Fly River, Papua New Guinea: Continental Shelf Research, v. 24, p. 2431-2454.

Hauck, T. E., Dashtgard, S. E., Pemberton, S. G. and Gingras, M. K. 2009 Brackish-water ichnological trends in a microtidal barrier island-embayment system, Kouchibouguac National Park, New Brunswick, Canada: Palaios, v. 24 (8), p. 478-496.

Hicks, D. M., Gomez, B. and Trustrum, N. A. 2004 Event suspended sediment characteristics and the generation of hyperpycnal plumes at river mouths: East coast continental margin, north island, New Zealand: J. Geology, v. 112, p. 471-485.

Krone, R. B. 1962 Flume studies of the transport of sediment in estuarial shoaling processes. Final Report, Hydraulic Engineering Laboratory and Sanitary Engineering Research Laboratory, University of California, Berkeley, USA.

Krone, R. B. 1993 Sedimentation revisited. In: Nearshore and Estuarine Cohesive Sediment Transport. Mehta, A. J. (ed.), American Geophysical Union, Coastal and Estuarine Studies, p. 108-125.

Lamb, M. P. and Mohrig, D. 2009 Do hyperpycnal-flow deposits record river flood dynamics: Geology (Boulder), v. 37 (12), p. 1067-1070.

Lau, Y. I. and Krishnappan, B. G. 1994 Does reentrainment occur during cohesive sediment settling?: J. Hydraul. Eng., v 120 (2), p. 236-244.

Mitchell, S. B., Lawler, D. M., West, J. R. and Couperthwaite, J. S. 2003 Use of continuous turbidity sensor in the prediction of fine sediment transport in the turbidity maximum of the Trent Estuary, UK: Estuarine, Coastal and Shelf Science, v. 58, p. 645-652.

Parchure, T. M. and Mehta, A. J. 1985 Erosion of soft cohesive sediment deposits: J. Hydraul. Eng., v. 111 (10), p. 1308-1326.

Sanford, L. P. and Halka, J. P. 1993 Assessing the paradigm of mutualy exclusive erosion and deposition of mud with examples from upper Chesapeake Bay: Mar. Geol., v. 114, p. 37-57

Shi, Z. and Kirby, R. 2003 Observations of fine suspended sediment processes in the turbidity maximum at the north passage of the Changjiang Estuary, China: J. Coastal Research, v. 19 (3), p. 529-540.

Uncles, R. J. and Smith, R. E. 2005 A note on the comparative turbidity of some estuaries of the americas.: J. Coastal Research, v. 21 (4), p. 845-852.

Winterwerp, J. C. 2006 On the Sedimentation rate of cohesive sediment, In: Maa, J. P.-Y., Sanford, L.P., Schoellhamer, D. H. (Eds.), Estuarine and Coastal Fine Sediment Dynamics, Elsevier, Amsterdam, p. 209-226.

Uncles, R. J., Stephens, J. A. and Law, D. J. 2006 Turbidity maximum in the macrotidal, highly turbid Humber Estuary, UK; flocs, fluid mud, stationary suspensions and tidal bores: Estuarine, Coastal and Shelf Science, v. 67 (1-2), p. 30-52.

FIG. 1. Distributions of salinity (fall average 1985-2006) and near-surface inorganic suspended solids (summer to fall average 1994) in Chesapeake Bay, USA. The salinity map ("chesapeake_bay_mean_surface_salinity_fall_1985_2006.pdf") is available from the Chesapeake Bay Program (www.chesapeakebay.net). The suspended sediment plot is reproduced from Fig 5a of Cerco et al, 2013.

FIG. 2. Experimental setup showing the side view of the tank filled to depth H with water having salinity S and clay concentration C. A camera (left) looks through the tank, which is lit from behind by a bank of lights (left) diffused by a white plastic sheet paper. The interior width of the tank is W and the distance from the front of the tank to the camera is L_c.

FIG. 3. Snapshots of clay settling in fresh water (left column) and in salt water (right column) each shown at three times during an experiment, as indicated. The descent of a front between clay-laden and clear water is evident in the salt water experiments.

FIG. 4. Vertical time series showing in false-colour (inset to (a)) the average intensity of light reaching the camera over time between the bottom and surface of the solution in the tank in four experiments with a) zero salinity, b) weak salinity and high clay concentration, c) high salinity and high clay concentration and d) high salinity and weak clay concentration. Light intensities near zero indicate high clay concentration whereas high intensities, near one, indicate low clay concentrations. For each time series values

of salinity (S) and clay concentration (C) are indicated in parts solute per thousand parts water by mass.

FIG. 5. Determination of the front descent rate and the virtual start time of the descent. The vertical time series shown in Figure 2d is reproduced as a gray scale image of intensity except in the band between z=7 cm and 8 cm, where a false-colour intensity scale is used as shown in the inset. White dashed lines are drawn along contours of constant intensity 0.28, 0.47, and 0.66. Solid black lines in the colour band show the lines best-fit between z=7 and 8 cm. These are extended as cyan-dashed lines to z=10 where the virtual start times are defined, as indicated by the three cyan-coloured circles.

FIG. 6. Measured speed of descent of the settling front as a function of salinity. Different symbols correspond to different clay concentrations as indicated.

FIG. 7. a) Virtual start time of front descent and b) linearly extrapolated time for complete settling. Both are plotted as a function of salinity with clay concentrations for both shown in the inset of a).

FIG. 8. Speed of front descent as a function of clay concentration averaged over experiments with salinities between 20 and 80 ppt. Inset shows a log-log plot of the same data.

FIGURE 1

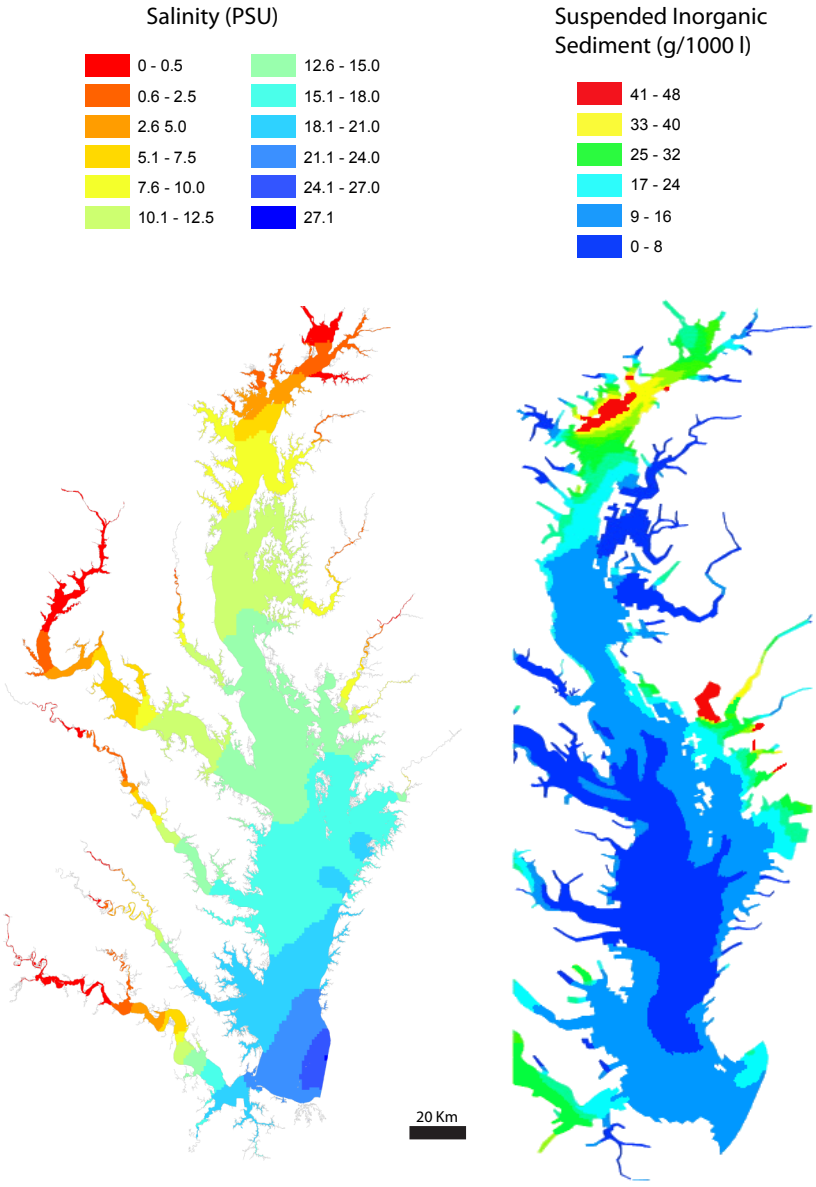
Salinity (PSU)
0 - 0.5
0.6 - 2.5
2.6 5.0
5.1 - 7.5
7.6 - 10.0
10.1 - 12.5
12.6 - 15.0
15.1 - 18.0
18.1 - 21.0
21.1 - 24.0
24.1 - 27.0
27.1
Suspended Inorganic Sediment (g/1000 l)
41 - 48
33 - 40
25 - 32
17 - 24
9 - 16
0 - 8
20 Km

FIGURE 2

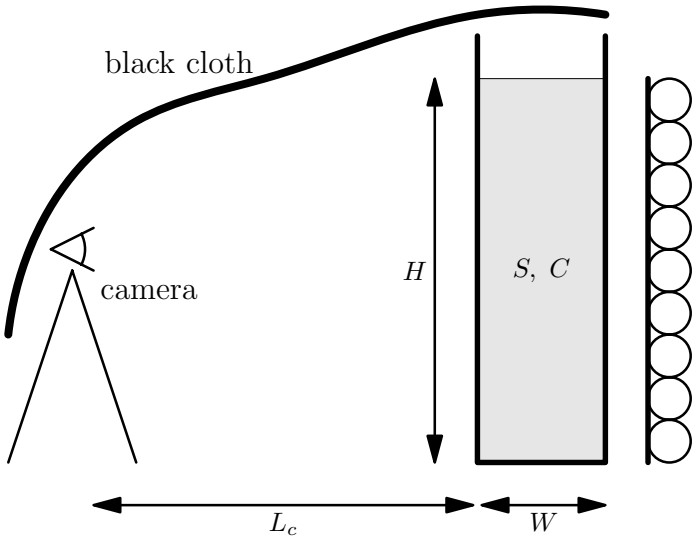

FIGURE 3

Clay Settling in Fresh Water

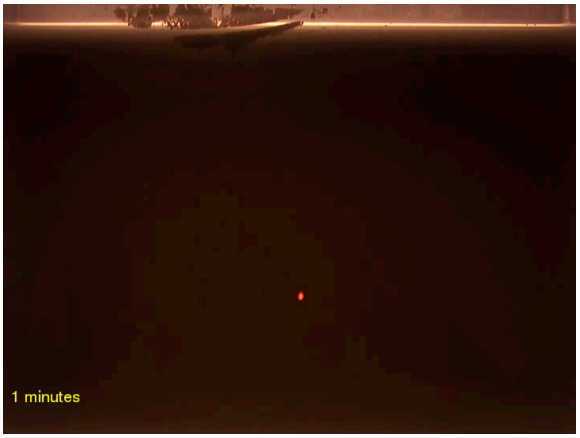

Clay Settling in Salt Water

FIGURE 4

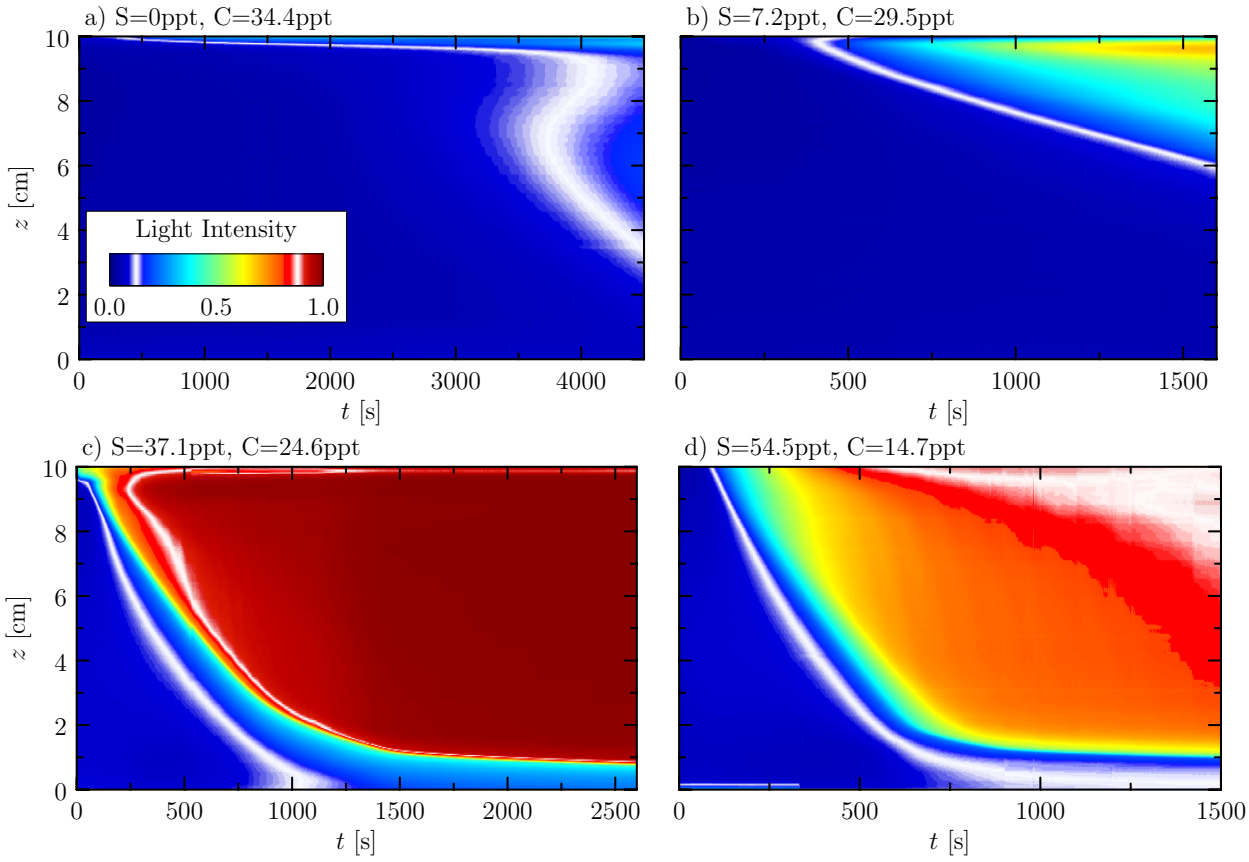
a) S=0ppt, C=34.4ppt
b) S=7.2ppt, C=29.5ppt
c) S=37.1ppt, C=24.6ppt
d) S=54.5ppt, C=14.7ppt
Light Intensity
0.0
0.5
1.0
z [cm]
t [s]

FIGURE 5

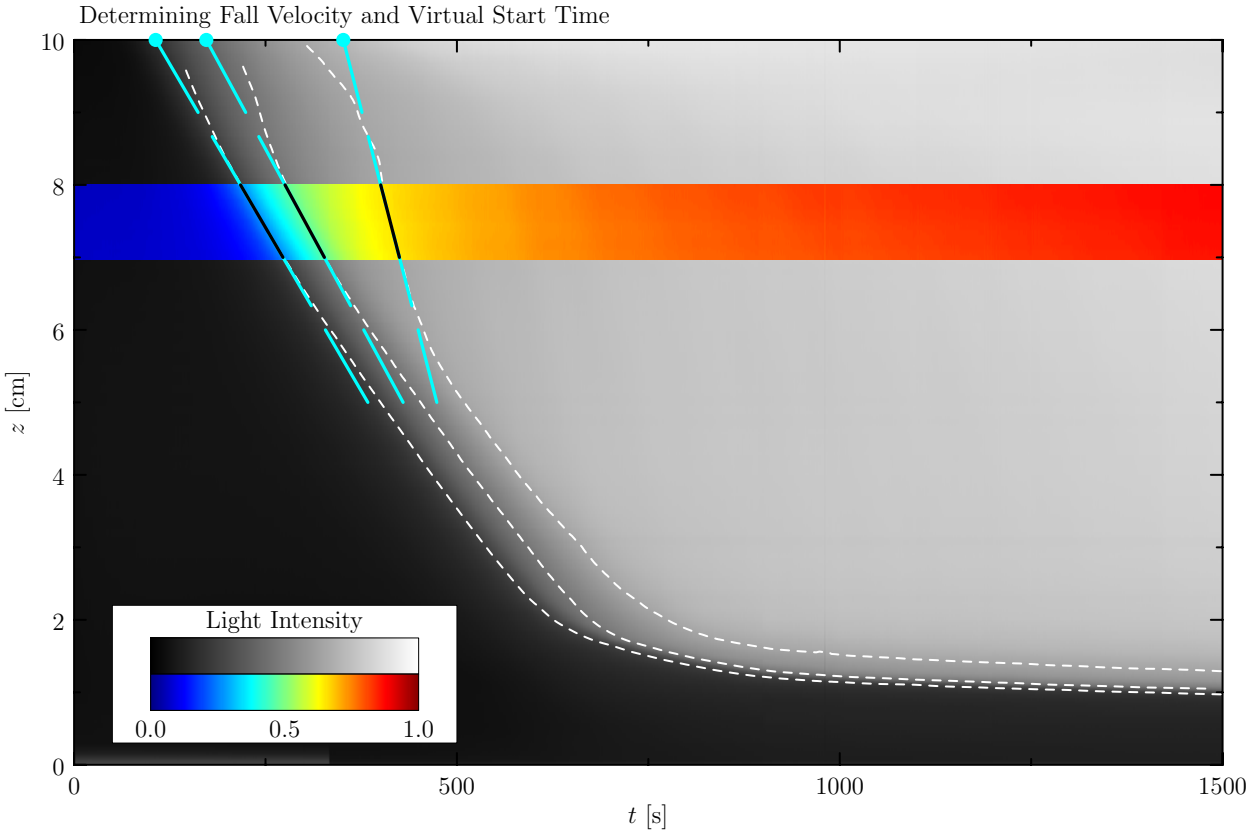
Determining Fall Velocity and Virtual Start Time
10
8
6
4
2
0
z [cm]
0
500
1000
1500
t [s]
Light Intensity
0.0
0.5
1.0

FIGURE 6

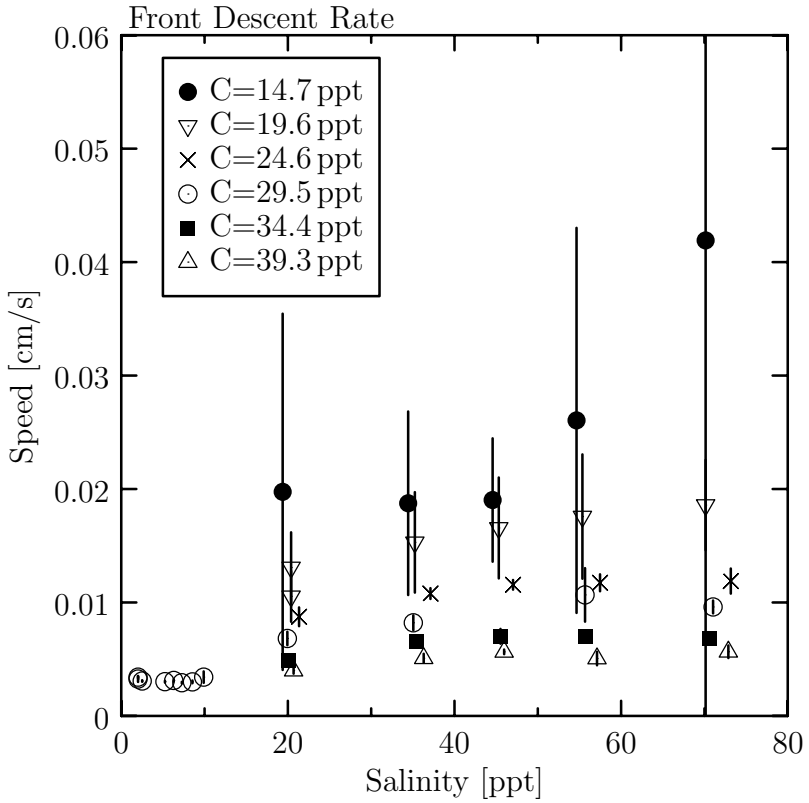
Front Descent Rate
C=14.7 ppt
C=19.6 ppt
C=24.6 ppt
C=29.5 ppt
C=34.4 ppt
C=39.3 ppt
Speed [cm/s]
Salinity [ppt]
0
0.01
0.02
0.03
0.04
0.05
0.06
0
20
40
60
80

FIGURE 7

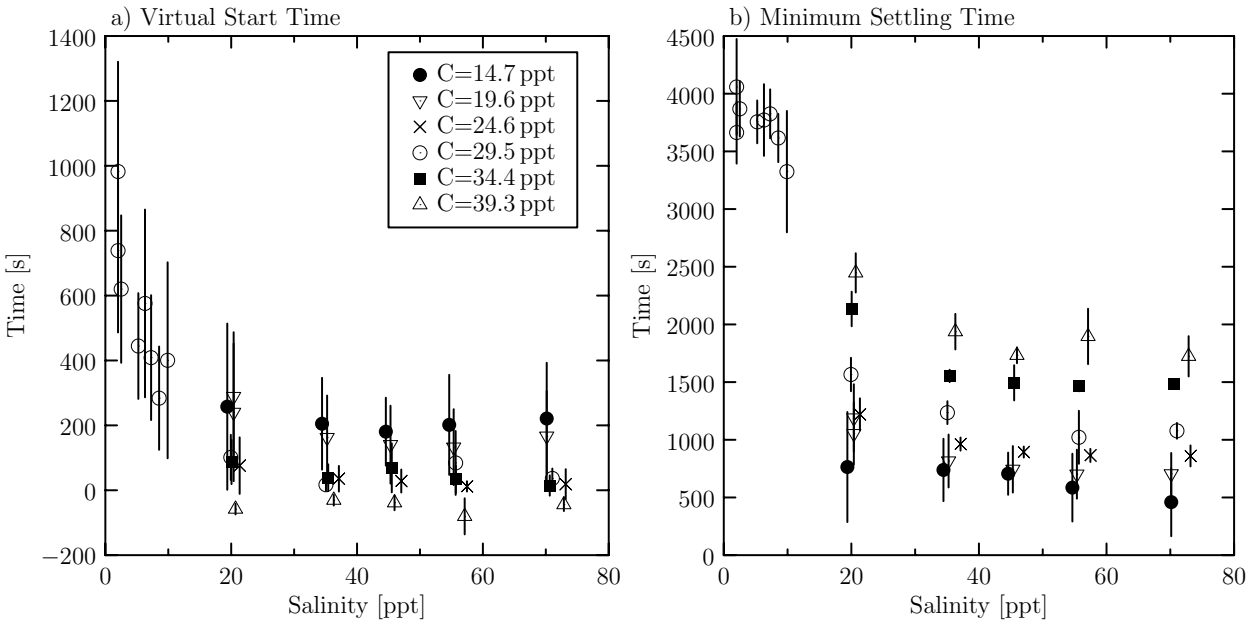
a) Virtual Start Time
b) Minimum Settling Time
C=14.7 ppt
C=19.6 ppt
C=24.6 ppt
C=29.5 ppt
C=34.4 ppt
C=39.3 ppt
Time [s]
Salinity [ppt]

FIGURE 8

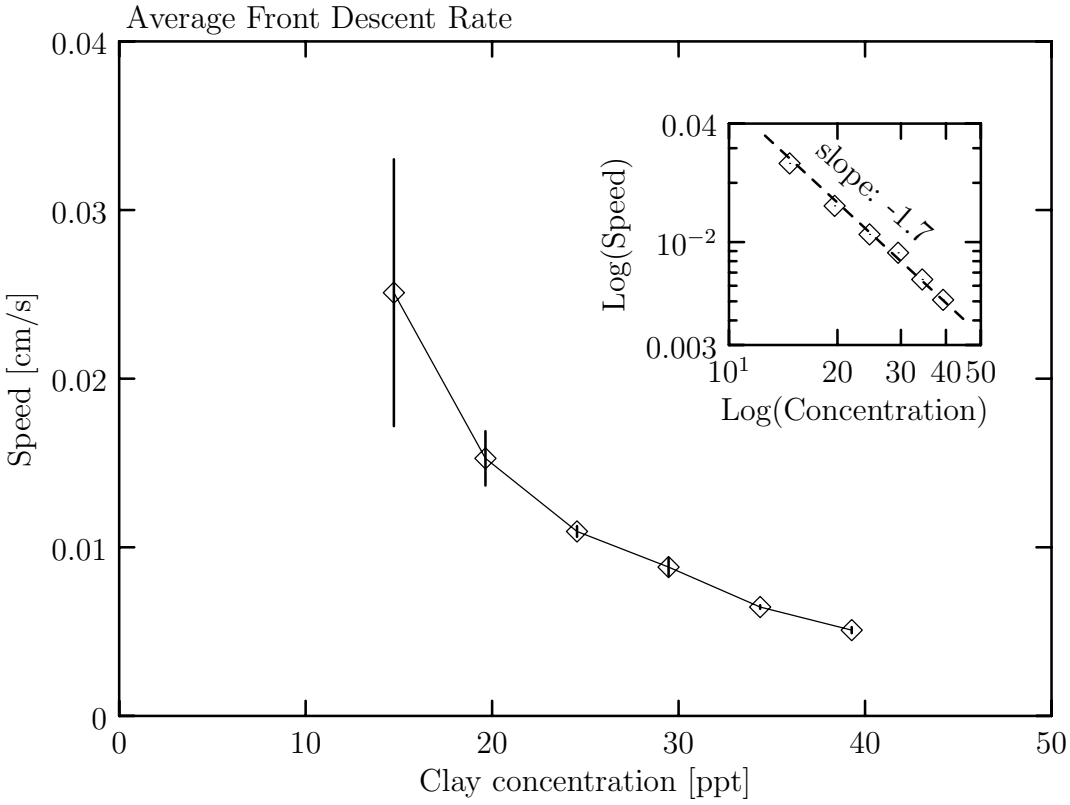
Average Front Descent Rate
Speed [cm/s]
Clay concentration [ppt]
0.04
0.03
0.02
0.01
0
0
10
20
30
40
50
Log(Speed)
Log(Concentration)
slope: -1.7
0.04
10^{-2}
0.003
10^{1}
20
30
40
50